Electrochemically Synthesized Ni@reduced Graphene Oxide Composite Catalysts for Hydrogen Evolution in Alkaline Media – the Effects of Graphene Oxide Support

Sanjin J. Gutić[1], Muharema Šabanović[1], Dino Metarapi[1], Igor A. Pašti[2], Fehim Korać[1], Slavko V. Mentus[2,3,]*

[1] University of Sarajevo, Faculty of Science, Department of Chemistry, Zmaja od Bosne 33-35, 71000 Sarajevo, Bosnia and Herzegovina
[2] University of Belgrade – Faculty of Physical Chemistry, Studentski trg 12-16, 11158 Belgrade, Serbia
[3] Serbian Academy of Sciences and Arts, Knez Mihajlova 35, 11000 Belgrade, Serbia
[*]E-mail: slavko@ffh.bg.ac.rs

Graphene-based materials and their role in electrocatalysis related to hydrogen production have been intensively investigated by many authors, often justified through a low price of such materials. In this study we used single-step electrodeposition/graphene oxide reduction route to prepare Ni@reduced-graphene-oxide composites for electrochemical hydrogen evolution reaction (HER). As the precursors for reduced graphene oxide, two different home-made graphene oxides were used. When compared to pure electrodeposited Ni, composite catalysts show improved catalytic activity which depends on Ni electrodeposition time in a volcano-type fashion. Using electrochemically prepared graphene oxide, HER overvoltage needed to reach 10 mA cm^{-2} was reduced to only -97 mV, showing the improvement by roughly 200 mV when compared to pure electrodeposited Ni. It was concluded that structural disorder and surface oxidation of graphene-based materials are the key properties for reaching high HER activities of such prepared catalysts. Based on this observation, it was discussed whether it is economically justified to use high quality graphene oxide for the preparation of HER catalysts, as the price (production and commercial) of this material can be extremely high, often exceeding the price of platinum.

1. INTRODUCTION

One of the mayor challenges in hydrogen economy is finding cheap but scalable systems for hydrogen production and storage. Water electrolysis of alkaline solutions provides relatively simple

route to obtain high purity hydrogen that can be used in fuel cells. The main drawback of this approach is the need for expensive catalytically active materials which, as a rule, are based on platinum group metals (PGM) [1-4]. For this reason, different PGM-free catalysts, relying on metals with moderate electrocatalytic activity and their alloys [5-9], metallic oxides [10,11], sulfides, phosphides [12], nitrides, carbides [10] and selenides [13] are intensively investigated to mitigate the aforementioned problem. In this way rather effective and durable PGM-free electrocatalysts were obtained.

Graphene-based nanomaterials are relatively new in experimental electrochemistry, but their unique properties are well recognized and applied in different electrochemical systems. Theoretical surface area of pristine graphene is 2630 m^2 g^{-1} which, together with a high electronic conductivity, make graphene-based materials excellent candidates for electrocatalyst supports [14]. However, some studies indicate that graphene not only enables good dispersion of catalytic particles, but takes an active part in an electrocatalytic process. This was particularly investigated for the case of electrochemical hydrogen evolution reaction (HER) [9,15,16], where improvements of catalytic activity were observed when graphene-based materials are used as catalyst supports. Significant promotion of catalytic activity of Ni electrodeposited on reduced graphene oxide (rGO) was explained in terms of the spillover of adsorbed H atoms at the Ni|rGO phase boundary. Such conclusion was derived due to the agreement between the experimental data and Kinetic Monte Carlo modelling of HER at supported catalysts using the HER mechanism which includes H spillover [16]. While such improvement of HER activity is very promising in terms of the identification of novel PGM-free catalysts, a big question regarding the source of graphene oxide (GO), which is used to prepare the composite catalyst, remains. Namely, there are different methods for the preparation of GO which differ greatly in terms of price and quality of the obtained GO [17]. In other words, maximization of catalyst effectiveness should be carefully balanced with its price to make it attractive for a large scale production.

In our previous study [16] we used commercially available GO for the preparation of Ni@rGO electrocatalysts. The price of such GO is actually higher than the price of platinum [18]. GO was used as a substrate for Ni electrodeposition during which it gets converted to rGO. A clear volcano-like dependency of the HER activity on the electrodeposition time, and conversely surface composition (i.e, Ni/C atomic ratio in the deposits) was observed. In this work we use the same procedure for the preparation of Ni@rGO catalytic surfaces, but with different homemade GO samples: graphene oxide prepared by chemical oxidation of graphite, and graphene oxide obtained by electrochemical oxidation of graphite. As will be discussed, these methods differ greatly by duration of the synthesis (chemical oxidation being rather time consuming) and quality of obtained GO (electrochemical exfoliation leading to relatively low quality of GO). We confirm that observed effects of formation of Ni|rGO interface on the HER activity are rather general, and discuss the effect of the preparation of GO on the electrocatalytic activity of Ni@rGO composites. Moreover, we critically address economic aspects of the use of graphene-based materials for the preparation of PGM-free HER catalysts.

2. EXPERIMENTAL

2.1. Preparation of graphene oxide samples

Chemically prepared graphene oxide was obtained from natural graphite flakes using modified Hummers method with ultrasonic exfoliation, described in details in Ref. [19]. The impurities were removed by successive rinsing with hydrochloric acid and water. Such obtained GO is designated hereafter as CGO (C for chemical), while its reduced form is designated as rCGO. Electrochemical oxidation and exfoliation was performed using graphite block, by adopting the procedure described in ref. [20]. Complete details about the synthesis are described in Ref. [21]. The obtained material is designated hereafter as EGO (E for electrochemical), while rEGO stands for its reduced form. Following the procedure as in Ref. [21] the concentration of GO samples in water/ethanol dispersions used for further experiments was set in such a way to give the same absorbance at 380 nm.

2.2. Preparation of Ni@rGO catalysts.

Ni@rGO catalysts were prepared by single step electrodeposition/GO reduction route described in Ref. [16]. In brief, GO dispersions in water/ethanol were drop-casted onto the precisely cut copper substrates (geometric area of 0.2826 cm^2). Mass of the GO substrate dropcasted on the Cu electrode was the same in all the samples. After vacuum drying, nickel deposition with the simultaneous reduction of GO was performed in a standard three-electrode cell by potentiostatic method. Potential of the working electrode was kept at −1.2 V *vs*. Ag/AgCl (KCl$_{satd.}$) during different time intervals, in order to deposit different amounts of nickel. All samples were denoted as Ni@r(C or E)GO"number", where the "number" denotes electrodeposition time in seconds (from 5 s to 100 s). We note that previous experience shows that electrochemical reduction of GO is very fast process, but highly dependent on the reduction potential. Importantly, for the minimum electrodeposition time (5 s) GO reduction is completed for the given Ni electrodeposition potential. Hence, in all the prepared Ni@rGO catalysts the rGO support was in the same state of reduction (for a given GO sample). Additionally, three reference samples were prepared. The first one is obtained by the electrodeposition of nickel onto the clean copper substrates and it is used to assess the improvement of HER activity when rGO is used as Ni support. The second reference sample is obtained by reduction of graphene without deposition of nickel and it was used to characterize the obtained rGO. Third reference sample is obtained by electrodeposition of Pt on clean Cu substrate. Deposition was done for 10 s, and this sample is used as a benchmark to compare catalytic activities of prepared Ni@rGO composite catalysts.

2.3. Characterization of materials

XRD patterns of GO samples were obtained using Ultima IV Rigaku diffractometer, equipped with Cu K$_{\alpha1,2}$ radiation source, using a generator voltage of 40.0 kV and a generator current of 40.0 mA. The range of 5–60° 2θ was used in a continuous scan mode with a scanning step size of 0.02° and at a scan rate of 2 ° min^{-1}. Raman spectra were collected on a DXR Raman microscope (Thermo

Scientific, USA) equipped with an Olympus optical microscope and a CCD detector. The laser beam was focused on the sample using objective magnification 50×. The scattered light was analyzed by the spectrograph with a 900 lines mm^{-1} grating. Power of the HeNe gas laser (excitation wavelength 633 nm) applied on the sample was kept at 2 mW. Scanning electron microscopy (SEM) with energy-dispersive X-ray spectroscopy (EDX) was performed using a JEOL JSM 6460 LV electron microscope, in order to obtain information about morphology and the surface chemical composition.

2.4. Electrocatalytic measurements

Electrocatalytic activity in 1 mol dm^{-3} aqueous KOH was investigated in standard three electrode cell, purged with ultrapure argon (99.999 vol.%) and connected to potentiostat/galvanostat PAR 263A controlled by PowerCV interface. Reference electrode was Ag/AgCl (KCl$_{satd.}$) (−0.197 V *vs*. SHE) and the counter electrode was Pt foil with the area of 1 cm^2. Potentials were re-calculated to the Reversible Hydrogen Electrode (RHE) scale and reported as such hereafter. Pseudostationary linear sweep voltammograms (LSV) were recorded at potential sweep rate of 10 mV s^{-1} in quiescent solution, with the constant overflow of Ar gas. Here we address only the effect of the rGO supports on the electrocatalytic activity towards the HER, without considering stability and durability of the catalysts. However, we note that catalyst degradation during the experiments was not observed in any of the cases.

3. RESULTS AND DISCUSSION

3.1. Graphene oxide characterization

XRD patterns of the chemically and electrochemically oxidized and exfoliated GO in aqueous suspension are shown in **Fig. 1**. Intensive reflection at $2\theta = 10.65°$ for the CGO sample indicate excellent separation of GO layers, with the interlayer distance larger than 8 Å [22]. This behavior is characteristic to GO with high degree of exfoliation [21]. There is, however, very weak and diffuse reflection at $2\theta = 28°$, arising probably due to a small fraction of remaining graphite in the obtained material. However, (002) graphitic reflection is dominant for the case of EGO, suggesting that electrochemical exfoliation is not as effective as the chemical one. Nevertheless, in the context of the discussion provided later, we note that it is much cheaper and does not require the use of aggressive chemicals. Also, electrochemical exfoliation takes minutes [20] over hours [19] (or days) needed for chemical exfoliation. An additional factor is possible contamination of GO by metals, like Mn, when using chemical exfoliation method, which requires special care regarding their removal. The GO yield of both methods could be rather small, with chemical exfoliation approach winning (in this particular case) over the electrochemical one.
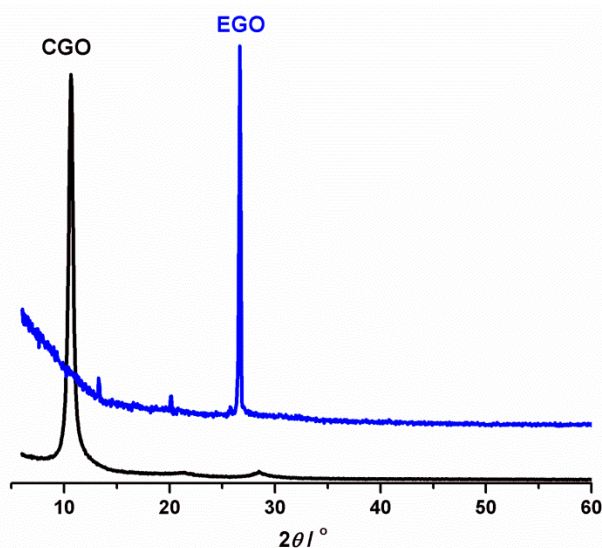
Figure 1. XRD patterns for graphene oxides prepared by chemical (CGO) and electrochemical (EGO) oxidation.

While XRD patterns differ to a great extent, Raman spectra of CGO and EGO (focused on characteristic region of D and G band, **Fig. 2**), are typical for GO prepared by oxidation of graphite. Characteristic intense peaks at ca. 1340 and 1600 cm^{-1} correspond to the D and G bands, respectively [23]. According to the D–to–G peak intensity ratios (I_D/I_G), high degree of structural disorder is present in the samples, as expected for the methods of preparation and types of graphite used for the oxidation. In order to further complement materials characterization, we refer to the previous work where FTIR spectra of analogously prepared CGO and EGO can be found [21], showing variety of surface oxygen functional groups.
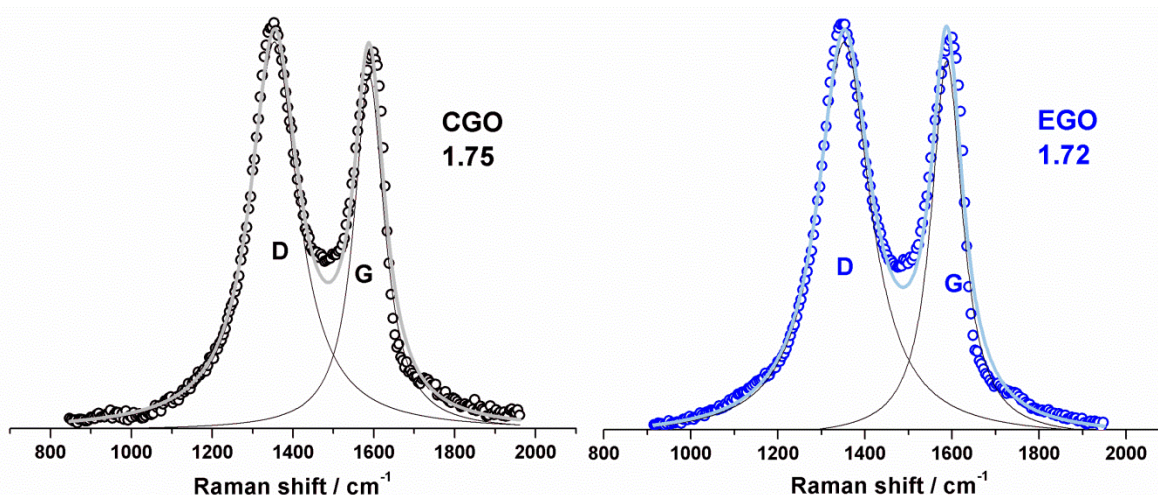

Figure 2. Raman spectra of prepared GO samples, with I_D/I_G ratios indicated in the figures. The values are obtained using the surfaces of D and G bands calculated upon the spectra deconvolution.

Additional EDX characterization indicated that EGO contains around 21 wt.% of O, while CGO has 44 wt.% of oxygen. Finally, we note that both CGO and EGO show typical irreversible

electrochemical reduction, suggesting a significant fraction of reducible oxygen moieties on the surface [21]. Based on the collected results of structural characterization, we propose that EGO sample is actually consisted of graphene nanoplatelets with heavily oxidized external surface and edge plane sites, while the interior of the nanoplatelets follows nearly graphitic stacking.

3.2. Characterization of Ni@r(C,E)GO surfaces and electrocatalytic activity

Ni@rGO samples were prepared by electrodeposition of nickel onto the GO-modified Cu substrate, with the concurrent reduction of GO substrate. Electrodeposition experiments were performed using deposition times of 5, 10, 30, 50 and 100 seconds. This leads to a gradual increase of the coverage of the underlying reduced (C or E)GO by Ni.
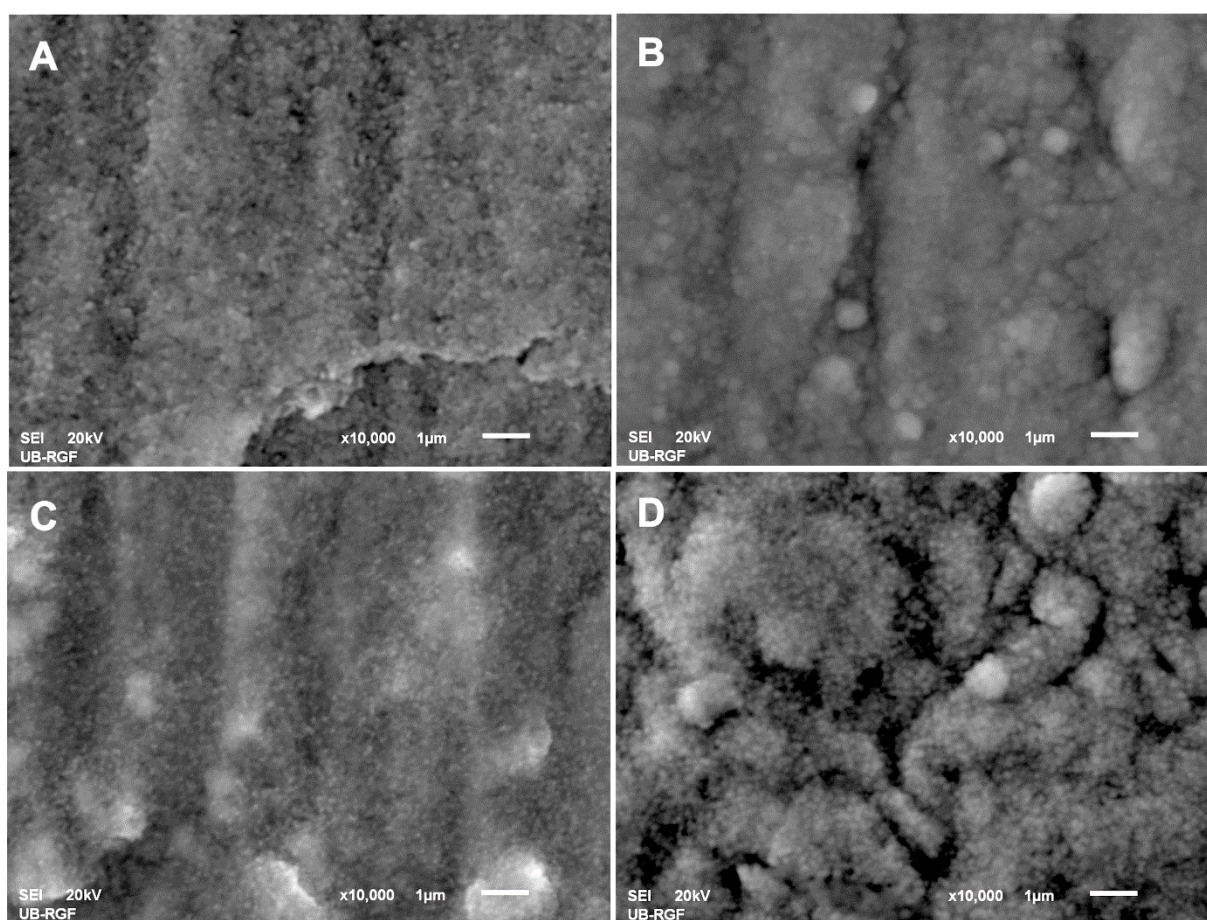

Figure 3. SEM images of Ni@rCGO30 (A), Ni@rCGO100 (B), Ni@rEGO30 (C) and Ni@rEGO100 (D) at common magnification of ×10000.

It was previously found that Ni atoms interact strongly with defects in graphene, with the adsorption energies of –7 eV for the case of the monovacanices, which is almost twice of the Ni cohesive energy [16]. This implies that the defects on (r)GO plane are the sites at which nucleation of Ni is preferred in the initial stages of electrodeposition. This is very important as we see that both CGO

and EGO have high concentration of defects (**Fig. 2**). However, during prolonged Ni electrodeposition, which was the case in described experiments, initial Ni deposits grow and start to coalesce over the underlying rGO phase, forming a well defined nickel deposit. SEM images of the samples obtained after 30 seconds of electrodeposition (**Fig. 3**) reveal granular morphology of Ni deposits, with fine and homogeneous coverage of rGO samples by Ni. There are no large Ni agglomerates suggesting the abundance of Ni|rGO phase boundaries in the samples obtained after 30 seconds of electrodeposition. According to the EDX analysis, atomic ratio of nickel to carbon in these samples was 0.45 ± 0.05, which is another good indication of the partial coverage of the rGO support by nickel. At higher deposition times nickel coalesce further, which ultimately leads to a complete coverage of the rGO support by uniform nickel deposit. This outcome is obvious from the images obtained for the samples prepared using the longest deposition time (100 s, **Fig. 3**, right). Morphology of the deposit points to the formation of large agglomerates, while the Ni/C atomic ratio for these samples, obtained by EDX, was over 1.7.

In agreement with our previous work [16], the samples prepared at intermediate electrodeposition times had the highest electrocatalytic activity towards the HER for both GO samples used as the support. Such behavior can be seen from the selected pseudostationary *j-E* curves shown in **Fig. 4** (for the cases where rCGO was used as the support) and **Fig. 5** (catalysts employing rEGO as the support). The effect of the electrodeposition time can be understood as a result of a balance between the number of catalytically active sites at which water discharge takes place (Ni), and the abundance of Ni|rGO interface, which boosts H_2 production *via* H_{ads} spillover [16]. We point to interesting features of Ni@rECGO slightly above 0 V *vs*. RHE which are not visible for short deposition times and cannot be ascribed separately to rCGO or Ni, but their unique combination. Observed behavior might be associated to enhanced water discharge and H_{ads} dynamics at Ni|rGO interface but detailed analysis cannot be provided at this point. In order to quantify HER activity, we follow recommendation given in ref. [6] and take the overpotential necessary to achieve the magnitude of current density of 10 mA cm^{-2} *per* geometric area as "the approximate current density expected for a 10% efficient solar-to-fuels conversion device under 1 sun illumination". When HER activity is expressed in such a way, a distinctive volcano-type relationship between HER activity and the amount of Ni in the composite catalyst (i.e. electrodeposition time) is obtained (**Fig. 4** and **5**, right panels). For the composites with the maximum catalytic activity (Ni@rCGO10 and Ni@rEGO30) it can be seen that HER commences basically at the equilibrium potential of hydrogen electrodes (0 V *vs*. RHE, vertical dashed lines in **Figs. 4** and **5**), just like in the case of the catalyst obtained by electrodeposition of Pt on Cu substrate. In the case of both graphene-based supports HER overpotential is reduced by approx. 200 mV, when compared to pure Ni electrodeposited directly on Cu support (black squares in **Figs. 5** and **6**).
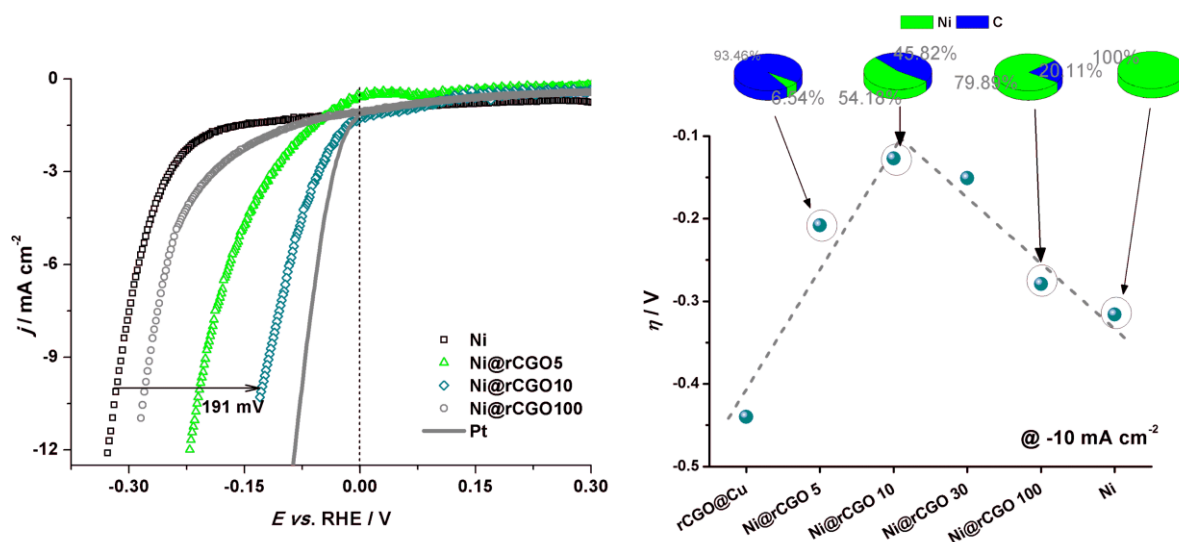
Figure 4. Left: Selected LSV curves for Ni@rCGO composite catalysts. LSV curve for Ni deposited on Cu is provided for reference (as a note, on rCGO-modified Cu electrode HER commences at potentials well below −0.3 V *vs*. RHE). Full line gives the LSV curve for Pt electrodeposited on Cu substrate (deposition time 10 s); right: volcano-type relationships between HER catalytic activity and Ni electrodeposition time. Ni-to-rGO support ration obtained by EDX is provided (in wt.%)

Figure 5. Left: Selected LSV curves for Ni@rECGO composite catalysts. LSV curve for Ni deposited on Cu is provided for reference. Full line gives the LSV curve for Pt electrodeposited on Cu substrate (deposition time 10 s); right: volcano-type relationships between HER catalytic activity and Ni electrodeposition time. Ni-to-rGO support ration obtained by EDX is provided (in wt.%)
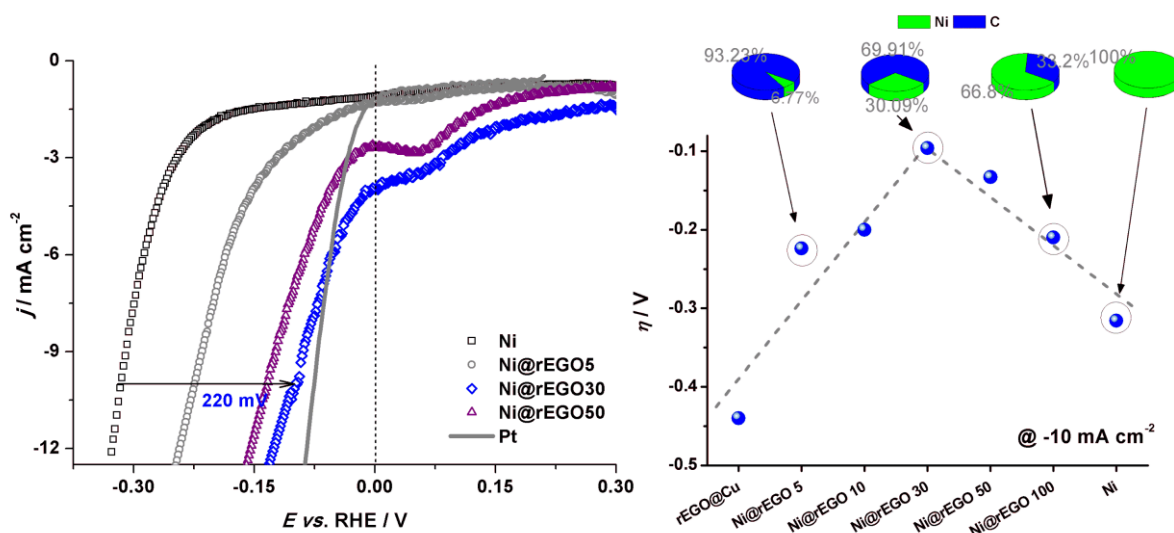
In order to put the obtained results in the proper context, we provide comparison with similar Ni-based HER electrocatalysts previously described in the literature and also with Pt as reference (**Table 1**). We note that a large list of PGM-free electrocatalysts can be found in ref. [6]. These

materials are binary or ternary systems consisted of Ni, Fe, Co, Mo and W (in different combinations). The Ni@rGO catalysts demonstrated here display HER activities which are comparable to some of the best bimetallic catalysts presented in ref. [6] but unambiguously beat their monometallic counterparts in terms of HER activity.

Table 1. HER overpotentials (η) for the graphene-supported Ni-based HER electrocatalysts reported previously in comparison with the activities of the catalyst prepared in this work.

| Material | η @ -10 mA cm^{-2} / mV | | Comment | Reference |
	pure Ni	Ni with rGO		
rGO@Ni	-380*	-120	rGO, deposited electrophoretically onto the Ni foam	[15]
Ni@rGO	-297^1 -187^2	-36	[1]Nickel substrate [2]Nickel foam on Ni substrate	[24]
Ni@rGO	-360	-290	Ni@rGO preparation procedure as in the present work, different GO substrate	[16]
NiMo@rGO	-175**	-120	NiMo alloy electrodeposited on Cu and GO-modified Cu substrates, respectively	[9]
Ni@rCGO	-316	-127	Ni deposited on GO prepared by Hummers method	This work
Ni@rEGO	-316	-96	Ni deposited GO prepared by electrochemical oxidation/exfoliation	This work
Pt	-45^1 -50^2		[1]Polished Pt disk [2]Platinized Pt disk	[6]
Pt	-76		Electrodeposited for 10 s on Cu substrate used for the preparation of Ni@rGO catalysts	This work

*HER overpotential recalculated from Hg/HgO reference electrode
**pure electrodeposited NiMo without rGO support

When the results presented here are compared with those from our previous work [16], it can be seen that the HER activity trends are identical – there is an optimum Ni deposition time which maximizes HER activity of Ni@rGO catalyst. However, there are two rather important differences. First, here we obtained maximum HER activity at smaller deposition times (10 s for CGO and 30 s for EGO) which means that lesser amounts of Ni can be used. Second, activity of the catalysts presented here is actually higher compared to the catalyst prepared using commercial GO sample in ref. [16] (**Table 1**). The full explanation of the link between the structure of the starting GO and the activity of

the final Ni@rGO composite is very difficult task, and we believe that definite conclusions are elusive at the moment. However, it is important to compare new findings with one more previous result. Namely, when Ni was deposited on so-called graphene nanoplatelets (GNP, commercial sample [25]) no HER activity improvement is observed, unlike in the case of GO [16]. According to the structural characterization, GNP has XRD pattern typical to that of graphite, very much like EGO (**Fig. 1**). However, its Raman spectrum shows exceptional structural order, with D band completely missing from the spectra, while oxygen content in the sample is almost negligible [16], which is opposite to the case of EGO (**Fig. 2**). When the results of the HER activity improvements are combined with the results of structural characterization of EGO and GNP, the key conclusion is that the surface oxidation and disorder are the main factors governing improved HER activity of Ni electrodeposited on graphene-based material, and not the exfoliation degree (as a note, commercial GO used in Ref. [16] has single layer ratio over 90%). In fact, the results presented here support this conclusion – slightly higher maximum HER activity was achieved for Ni@rEGO than Ni@rCGO. However, we note that the optimal rGO-to-Ni ratio depends on the exact properties of GO used to prepare catalysts.

Discussion provided above motivates the analysis of the cost-related aspect of the preparation of ~~the~~ graphene-containing catalysts for HER. EGO is expected to be much cheaper than CGO due to significantly simpler and much shorter (time-wise) synthesis procedure. Speaking of the price estimate for homemade CGO, about 15 EUR is necessary only for the analytical-grade chemicals (excluding graphite), needed for the treatment of 1 g of graphite by applied modified Hummers methods (with phosphoric acid). When compared with the price of metallic platinum (ca. 24 EUR *per* gram on March 4th 2019, and a 5-year average of around 36 EUR *per* gram [26]), taking into account that yield of the reaction could be low [27] and that further steps are needed (i.e., purification, sonication, etc.), 1 g of chemically prepared GO costs nearly as 1 g of Pt. On the other hand, aqueous electrochemical approach for graphite oxidation/exfoliation demands the use of only one chemical reagent (i.e. electrolyte, most often H_2SO_4), and relatively small amount of electrical energy. Anodic exfoliation is usually done for short periods of time (up to 5 minutes) under the DC voltage of 10 V across the cell, with very low current flow [28], while exfoliation efficiency can be significantly improved with simple pretreatments [29]. Also, the absence of $KMnO_4$ in the synthetic route excludes extensive purification of the obtained material, which further reduces large-scale preparation costs. Taking into consideration our conclusions from the preceding discussion that the exfoliation degree is not determining factor in the active role of graphene-based supports in HER electrocatalysis, electrochemical approach seems to be economically more justified. Also, as the quality of GO is not definite factor for maximizing catalytic activity, it might also be speculated that other types of carbons could be used for the same purpose, if structural disorder and oxidation degree could be properly engineered.

4. CONCLUSIONS

We prepared two series of Ni@rGO composite catalysts for HER in alkaline media using two different GO samples. Catalyst preparation involved a single step electrodeposition of Ni during which GO support is converted to rGO. Considering the activity of the catalysts it was observed that there is

an optimal Ni deposition time for each GO which results with maximum HER activity. High activities of prepared catalysts were observed, and the HER overpotential required to reach 10 mA cm^{-2} was reduced to only −96 mV when using EGO obtained by anodic electrochemical exfoliation of graphite. For comparison, the overvoltage for prepared Pt catalyst was −76 mV. These results compared very well with some of the best metallic PGM-free catalysts reported so far. However, another result which has to be outlined is the fact that the improvement of the catalytic activity of Ni is apparently not linked to the quality of GO and the exfoliation degree, but to surface oxidation and disorder. It seems that relatively cheap EGO performs much better than more expensive alternatives obtained by chemical exfoliation. This result also suggests that other forms of carbon could also be used for the same purpose if their surface properties are tailored in a proper way. Yet, the questions of the right structural disorder and the concentration of reducible oxygen functional groups which provide the best HER activity remain open.

References

1. A. Eftekhari, *Int. J. Hydrogen Energy*, 42 (2017) 11053.
2. P.C.K. Vesborg, B. Seger and I. Chorkendorff, *J. Phys. Chem. Lett.*, 6 (2015) 951.
3. F. Safizadeh, E. Ghali and G. Houlachi, *Int. J. Hydrogen Energy*, 40 (2015) 256.
4. M. Carmo, D.L. Fritz, J. Mergel and D. Stolten, *Int. J. Hydrogen Energy*, 38 (2013) 4901.
5. J.M. Jakšić, M.V. Vojnović and N.V. Krstajić, *Electrochim. Acta* 45 (2000) 4151.
6. C.C.L. McCrory, S. Jung, I.M. Ferrer, S.M Chatman, J.C. Peters and T.F. Jaramillo, *J. Am. Chem. Soc.*, 137 (2015) 4347.
7. T. Wang, X. Wang, Y. Liu, J. Zheng and X. Li, *Nano Energy*, 22 (2016) 111
8. Q. Zhang, P. Li, D. Zhou, Z. Chang, Y. Kuang and X. Sun, *Small*, 13 (2017) 1701648.
9. S.J. Gutić, A.Z. Jovanović, A.S. Dobrota, D. Metarapi, L.D. Rafailović, I.A. Pašti and S.V. Mentus, *Int. J. Hydrogen Energy*, 43 (2018) 16846
10. Y. Zhang, J. Zang, C. Han, S. Jia, P. Tian, H. Gao and Y. Wang, *Int. J. Hydrogen Energy*, 42 (2017) 26985
11. N. Danilovic, R. Subbaraman, D. Strmcnik, K.C. Chang, A.P. Paulikas, V.R. Stamenkovic and N.M. Markovic, *Angew. Chem., Int. Ed.*, 51 (2012) 12495
12. P. Guo, Y.-X. Wu, W.-M. Lau, H. Liu and L.-M. Liu, *Int. J. Hydrogen Energy*, 42 (2017) 26995
13. D. Kong, H. Wang, Z. Lu and Y. Cui, *J. Am. Chem. Soc.*, 136 (2014) 4897
14. C. Wang and D. Astruc, *Prog. Mater. Sci.*, 94 (2018) 306
15. D. Chanda, J. Hnát, A.S. Dobrota, I.A. Pašti, M. Paidar and K. Bouzek, *Phys. Chem. Chem. Phys.*, 17 (2015) 26864
16. S.J. Gutić, A.S. Dobrota, M. Leetma, N.V. Skorodumova, S.V. Mentus and I.A. Pašti, *Phys. Chem. Chem. Phys.*, 19 (2017) 13281
17. A.C. Ferrari, F. Bonaccorso, V. Fal'ko, K.S. Novoselov, S. Roche, P. Bøggild, S. Borini, F.H.L. Koppens, V. Palermo, N. Pugno, J.A. Garrido, R. Sordan, A. Bianco, L. Ballerini, M. Prato, E. Lidorikis, J. Kivioja, C. Marinelli, T. Ryhänen, A. Morpurgo, J.N. Coleman, V. Nicolosi, L. Colombo, A. Fert, M. Garcia-Hernandez, A. Bachtold, G.F. Schneider, F. Guinea, C. Dekker, M. Barbone, Z. Sun, C. Galiotis, A.N. Grigorenko, G. Konstantatos, A. Kis, M. Katsnelson, L.

Vandersypen, A. Loiseau, V. Morandi, D. Neumaier, E. Treossi, V. Pellegrini, M. Polini, A. Tredicucci, G.M. Williams, B.H. Hong, J.-H. Ahn, J.M. Kim, H. Zirath, B.J. van Wees, H. van der Zant, L.i Occhipinti, A. Di Matteo, I.A. Kinloch, T. Seyller, E. Quesnel, X. Feng, K. Teo, N. Rupesinghe, P. Hakonen, S.R.T. Neil, Q. Tannock, T. Löfwander and J. Kinaret, *Nanoscale*, 7 (2015) 4598

18. https://www.acsmaterial.com/graphene-oxide-s-method-1426.html. [Accessed 3 March 2019].
19. D.C. Marcano, D.V. Kosynkin, J.M. Berlin, A. Sinitskii, Z. Sun, A. Slesarev, L.M. Alemany, W. Lu and J.M. Tour, *ACS Nano*, 4 (2010) 4806.
20. J.M. Munuera, J.I. Paredes, S. Villar-Rodil, M. Ayán-Varela, A. Pagán, S.D. Aznar-Cervantes, J.L. Cenis, A. Martínez-Alonso and J.M.D. Tascón, *Carbon*, 94 (2015) 729
21. S.J. Gutić, D.K. Kozlica, F. Korać, D. Bajuk-Bogdanović, M. Mitrić, V.M. Mirsky, S.V. Mentus and I.A. Pašti, *Phys. Chem. Chem. Phys.*, 20 (2018) 22698
22. L. Stobinski, B. Lesiak, A. Malolepszy, M. Mazurkiewicz, B. Mierzwa, J. Zemek, P. Jiricek and I. Bieloshapka, *J. Electron. Spectros. Relat. Phenomena*, 195 (2014) 145
23. S. Claramunt, A. Varea, D. López-Díaz, M. Mercedes Velázquez, A. Cornet and A. Cirera, *J. Phys. Chem. C*, 119 (2015) 10123
24. L. Wang, Y. Li, M. Xia, Z. Li, Z. Chen, Z. Ma, X. Qin and G. Shao, *J. Power Sources*, 347 (2017) 220
25. http://www.acsmaterial.com/graphene-nanoplatelets-2-10nm-846.html. [Accessed 3 March 2019].
26. https://www.kitco.com/charts/liveplatinum.html. [Accessed 4 March 2019].
27. E.J. Frankberg, L. George, A. Efimov, M. Honkanen, J. Pessi and E. Levänen, *Fuller. Nanotub. Car. N*, 23 (2015) 755
28. J.I. Paredes and J.M. Munuera, *J. Mater. Chem. A*, 5 (2017) 7228
29. J.M. Munuera, J.I. Paredes, S. Villar-Rodil, A. Martínez-Alonso and J.M.D. Tascón, *Carbon*, 115 (2017) 625.